A scalable high-porosity wood for sound absorption and thermal insulation

Xinpeng Zhao ®[1,10], Yu Liu[1,10], Liuxian Zhao[2,10], Amirhossein Yazdkhasti[2], Yimin Mao[1,3], Amanda Pia Siciliano ®[1], Jiaqi Dai[4], Shuangshuang Jing[1], Hua Xie ®[1], Zhihan Li[1], Shuaiming He ®[1], Bryson Callie Clifford ®[1], Jianguo Li[1], Grace S. Chen[1], Emily Q. Wang[1], Andre Desjarlais[5], Daniel Saloni ®[6], Miao Yu[2], Jan Kośny[7], J. Y. Zhu ®[8], Amy Gong[4] & Liangbing Hu ®[1,9] ✉

The search for more-sustainable materials has motivated research on lightweight, porous structures for thermal insulation and noise reduction, such as for construction and cold-chain transportation. Wood, known as one of the most renewable materials on Earth, has been widely and long used in construction for its high strength/weight ratio, wide abundance, low cost and relative sustainability. However, natural wood is much less effective at reducing noise or preventing heat loss than conventional petroleum- and mineral-based porous structures (for example, expanded polystyrene foam and mineral wool). Here we report the extraordinary noise-reduction and thermal-insulation capabilities of a scalable, high-porosity wood structure, 'insulwood', fabricated by removing lignin and hemicelluloses from natural wood using a rapid (~1 h) high-temperature process followed by low-cost ambient drying. Insulwood demonstrates a high porosity of ~0.93, a high noise-reduction coefficient of 0.37 at a frequency range of 250–3,000 Hz (for 10-mm-thick wood), a low radial thermal conductivity of 0.038 W m^{-1} K^{-1} and a high compressive strength of ~1.5 MPa at 60% strain. Furthermore, this new wood-based material can be rapidly processed into a vacuum insulation panel (~0.01 W m^{-1} K^{-1}) for thermal insulation applications with limited space (for example, refrigerators, cold-chain transportation and older buildings). The material is unique in its combination of renewable source materials, high porosity, high sound absorption, low thermal conductivity and high mechanical robustness, as well as in its efficient, cost-effective and scalable manufacturing. These attributes make insulwood promising as a sustainable construction material for improved noise and thermal regulation.

In the United States, buildings account for ~40% of energy consumption and are the source of ~38% of carbon dioxide (CO_2) emissions[1]. Reducing both the embodied CO_2 that is emitted during the life cycle of building materials and the operational energy consumption of heating, ventilation and air conditioning systems would play a critical role in minimizing CO_2 emissions. An additional problem associated with buildings is the noise from road traffic, construction sites and social activities, which can affect the health and well-being of residents. Therefore, developing a high-performance multifunctional construction material that can both block sound transport and retard heat loss through walls and roofs is key for improving occupant comfort and lowering carbon footprints. High-porosity structures (>0.9) can effectively

attenuate sound energy by increasing the air–pore wall friction[2] as well as decrease thermal transport by reducing the material's cross-sectional solid area and increasing the tortuosity of heat transfer pathways[3–6]. Currently, due largely to their low price, the commercial market for thermal-insulation and sound-absorption materials is dominated (>90% of the market share[7]) by porous structures that are produced from petroleum-based polymers (for example, polyurethane foams and expanded/extruded polystyrene foams) and rock- and slag-based fibres (for example, mineral wools and glass wools)[8–10]. However, these synthetic porous materials rely on non-renewable sources and generate pollutants during manufacturing (for example, SO_x and NO_x)[11]. In addition, the fabrication of these traditional construction materials may involve high-temperature processes, which produce substantial carbon emissions[10,12,13]. The disposal or landfill of the synthetic materials, especially polymer foams, at the end of use can cause environmental issues[7,14]. Replacing such carbon-intensive, non-renewable, synthetic porous materials with renewable biomass-based structures could lead to a 16% reduction of embodied carbon in buildings[15], which would be a notable improvement from an environmental standpoint. However, factors such as scalability and cost must be overcome to make such biomass-based alternatives a reality.

Wood is a renewable structural material that has been used in construction for thousands of years due to its excellent mechanical strength, natural abundance and low cost[16]. Recently, wood has also emerged as an important sustainable building material due to its processability, renewability and biodegradability[16]. However, due to its relatively low porosity compared with commercial porous structures and strong covalent bonds between the cellulosic polysaccharides (cellulose and hemicelluloses) and lignin of the wood cell walls, natural wood features a radial thermal conductivity of 0.1–0.4 W m^{-1} K^{-1}, which prevents it from effectively reducing heat loss[17,18]. In addition, natural wood (without artificial pores[19]) is sound reflective and therefore a poor noise absorber[20–22]. The addition of pores (or voids) has shown to be an effective way to increase sound dissipation and decrease the thermal conductivity of solid materials since pores increase the tortuosity of heat and sound transfer paths[2,4]. Recent studies have begun to develop porous wood-based materials via 'top-down' processes, including various chemical treatments[16,23–28] and fungal decay[29]. For example, Wang and co-workers[24] prepared a porous spongy wood from natural balsa by selectively removing lignin (NaClO₂, 100 °C for 6 h) and hemicelluloses (NaOH, 80 °C for 8 h), followed by freeze drying at −56 °C for 36 h. Similarly, Hu and co-workers[25] transformed bulk natural balsa into a porous wood aerogel using a delignification process (NaOH/Na₂SO₃ and H₂O₂) at 100 °C for more than 5 h, followed by freeze drying (~24 h). Although these top-down methods start with low-cost raw materials and require only one or two procedures, they suffer from several drawbacks, including long processing times (several days to several weeks) and expensive drying processes (for example, freeze drying)[24–26,29]. Drying at ambient pressure and temperature would be simpler, more cost effective and energy saving. However, directly drying water-filled cellulose-based materials generally causes structural collapse due to fiber hornification and hydrogen bonding, leading to a densified structure and not the desired porous morphology[30,31]. In addition, state-of-the-art porous wood-based materials[24–26,29] suffer from weak mechanical robustness as the wood cell structures are severely destroyed during the delignification process. As a result, it has remained challenging to fabricate robust high-porosity cellulose-based materials in a scalable, fast and cost-effective way.

In this Article, we report a rapid and cost-effective top-down approach that applies a fast high-temperature delignification technique to natural wood, followed by low-cost ambient pressure drying, to produce a highly porous cellulose-based structure with the natural structure retained that we call 'insulwood' (Fig. 1a). Insulwood exhibits a high porosity of >0.93, a high noise-reduction coefficient of 0.37 at a frequency range of 250–3,000 Hz (for a 10-mm-thick wood sample),

a low thermal conductivity of 0.038 W m^{-3} K^{-1} and a high compressive strength of 1.5 MPa (60% compression) due to the retention of the original hierarchical wood structure. We also showed the heat transfer inside the insulwood can be further suppressed by sealing and vacuuming air from the material to form a highly insulated vacuum insulation panel (VIP; Fig. 1a), enabling a low thermal conductivity of ~0.01 W m^{-1} K^{-1}, which is approximately one-third lower compared with stationary air (~0.026 W m^{-1} K^{-1}, 300 K, 1.0 atm). As a result of the aligned pores inherited from the natural wood starting material, the outgassing rate of the insulwood is twice as fast as that of expanded polystyrene foams, which feature random pores, thus decreasing the time and energy needed to fabricate the panel. Most importantly, this fabrication process is compatible with existing infrastructures for delignification, chemical recovery methods and wastewater treatment in the pulp and paper industry[32,33], simplifying transition into industrial manufacturing. Therefore, this work demonstrates a sustainable and scalable insulation material for walls, roofs and floors that can improve residential comfort in terms of decreased thermal and sound transfer as well as provide enormous potential environmental benefits.

Results and discussion
Insulwood preparation and its structure characteristics

To prepare the insulwood (Fig. 2a), we selected natural paulownia wood (*Paulownia tomentosa*, density of 0.25–0.30 g cm^{-3}, cut along the growth direction) as a starting material for its fast growth rate and high biomass production (up to 50 t ha^{-1} yr^{-1}) (refs. 34,35). Although recently developed in situ delignification techniques at 100 °C (ref. 23) can remove lignin and hemicelluloses from natural wood, most earlier studies[24–26] required multiple steps and sulfur-containing chemicals (for example, Na₂SO₃ and Na₂S), resulting in long processing time (~5–10 h) (Fig. 2b). As an alternative, we used ~5.0 wt% NaOH aqueous solution for delignification (a sulfur-free soda process[36]) under higher temperature. The high-temperature condition helps to rapidly remove lignin and hemicelluloses through various chemical reactions (for example, β–O–4 bond cleavage of lignin, peeling and alkaline hydrolysis of hemicelluloses) within 1.0 h, which is more than ten times faster than current state-of-the-art methods[24–26,29]. In addition, this approach retains the desired natural structure of the hierarchically aligned cellulose fibres, allowing delignified wood to achieve a good mechanical strength. The water permeated in the porous wood structure during delignification is then replaced by ethanol with low surface tension, which prevents pore collapse on removal when dried under ambient conditions (see details in Supplementary Figs. 1–6). Furthermore, we then completely dried the delignified wood under ambient conditions to obtain the final insulwood product in just 7.0 h, which is much faster than freeze drying (Fig. 2b).

As shown in Fig. 2c,d and Supplementary Fig. 7, natural paulownia wood features a honeycomb-like cellular structure with thin cell walls that make up the vertically aligned tracheids (pore size of 20–50 μm) and large vessels (pore size of 100–200 μm) of the wood structure. The cell walls are composed primarily of cellulose microfibre bundles bound within a matrix of lignin and hemicelluloses[37]. After the delignification treatment and drying, the morphology and structure of the resulting insulwood change remarkably compared with the starting material. Figure 2e,f and Supplementary Fig. 8 show that numerous small voids (<10 μm) are generated between neighbouring wood cell walls (in the middle lamella region) due to detachment by the removal of the lignin/hemicelluloses matrix, resulting in an increased structural porosity. We confirmed lignin removal by comparing the Fourier transform infrared (FTIR) spectra of the natural wood with the insulwood (Fig. 2g), where characteristic lignin peaks at 1,593, 1,504 and 1,462 cm^{-1} (aromatic skeletal vibrations) disappeared after the chemical treatment. The loss of the peaks at 1,737 and 1,236 cm^{-1} show that hemicelluloses in natural wood was also removed by the delignification treatment. In addition, we conducted a chemical analysis that
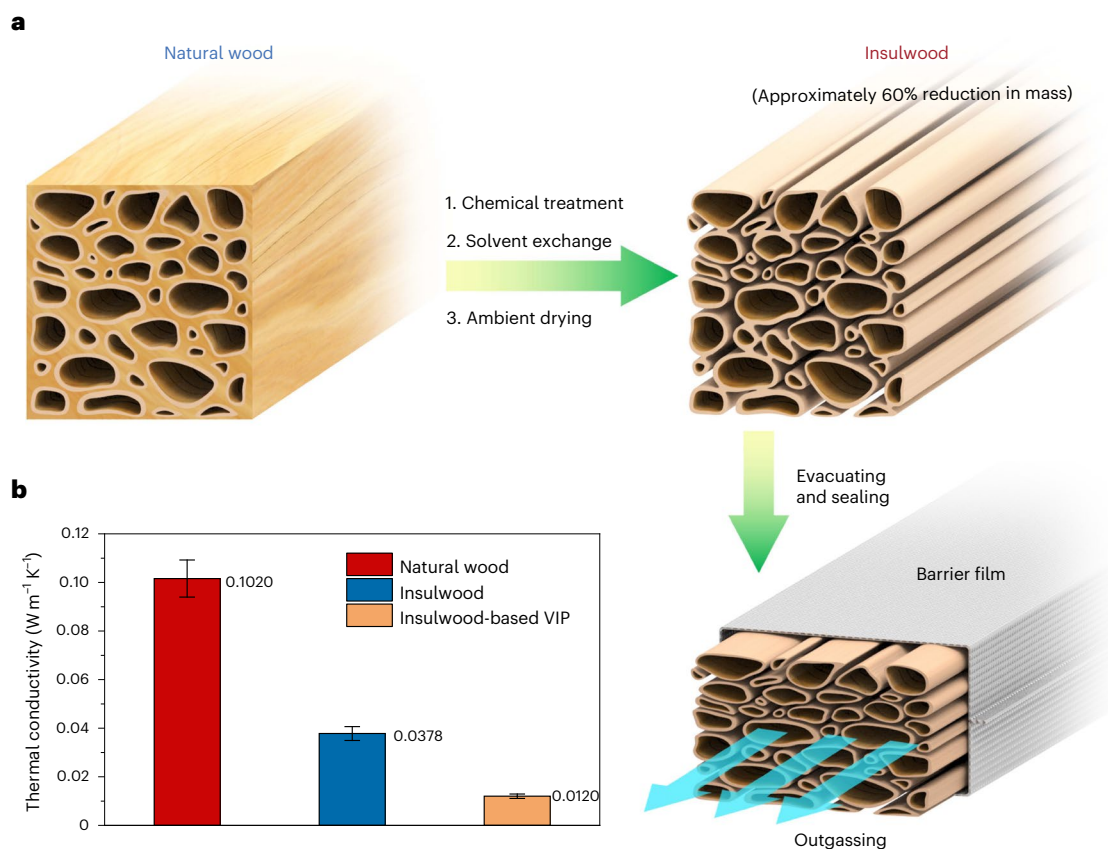
Fig. 1 | The fabrication and thermal performance of insulwood and insulwood-based VIPs. a, Schematic of the changes of wood pore structures after rapid high-temperature delignification and in an insulwood-based VIP. Removal of lignin and hemicelluloses can remarkably increase the porosity of the wood, which is beneficial for thermal insulation and sound absorption, while still retaining the naturally aligned structure of the wood channels, maintaining a high mechanical performance. The insulwood is enveloped by an air- and water-vapour-tight barrier layer. The open and aligned pores allow the gas inside the insulwood to evacuate quickly, creating a vacuum that helps suppress heat conduction by the air. Note that the volumetric shrinkage of the insulwood sealed in the gas barrier envelope is ~25%. **b**, Comparison of the thermal insulation performances of natural wood (0.102 ± 0.008 W m^{-1} K^{-1}), insulwood (0.0378 ± 0.003 W m^{-1} K^{-1}) and VIPs (0.0120 ± 0.0009 W m^{-1} K^{-1}) fabricated using insulwood. The thermal conductivity of insulwood is comparable to most commercial porous materials, such as expanded polystyrene and glass wool[45]. All data were analyzed from three independent measurements; error bars show s.d.

further showed the lignin and hemicelluloses were almost completely removed after the delignification process (Supplementary Fig. 9). We also conducted two-dimensional wide-angle X-ray scattering (WAXS) to analyze the crystal polymorphism of insulwood (Supplementary Fig. 10); the WAXS indicates that the cellulose I maintains its structure and a portion of the cellulose Iβ increases during our high-temperature delignification process. As a result of delignification, the density of insulwood is ~40% that of the natural wood (Fig. 2h), increasing the porosity from ~80% to ~93%. Note that we evaluated the porosity of natural woods and insulwood on the basis of their weights and volumes, and the wood cell wall density is assumed to be 1.5 g cm^{-3} (refs. 38,39).

Sound-absorption performance of the insulwood

The sound-absorption performance of wood is determined mainly by its surface structure and the characteristics of the internal pores[21]. Although natural woods have abundant pores, their sound-absorption performance is poor due to the hard and dense surface and low number of continuous pores[21,22]. After delignification, numerous millimetre-scale cracks (1–5 mm long) were formed uniformly on the surface of insulwood (Supplementary Fig. 11) due to the detachment of the wood cell walls after the high-temperature chemical treatment (Fig. 2e,f). These cracks allow more incident sound waves to penetrate the material, functioning as sound-absorbing pores. In addition, the delignification treatment generates numerous interconnected small

pores (<10 μm, in the middle lamella region) between the cell walls (Fig. 2e,f), which provide tortuous pathways for sound-wave dissipation via the air–cell wall friction. Removing the lignin and hemicelluloses also considerably decreases the mechanical strength of the wood cell walls, which allows sound waves to be converted into mechanical and thermal energy through resonances of the wood cell walls.

To explore whether these structural changes did impact the sound transport, we used a two-microphone transfer function method[40] to measure the sound-absorption coefficient of insulwood (Fig. 3a and Supplementary Fig. 12) at a frequency range of 250–3,000 Hz. For a 10-mm-thick piece of the insulwood, we found a relatively large sound-absorption coefficient of 0.2 in the frequency range of 250–1,250 Hz, which sharply increased to ~0.75 as the frequency increased to 2,500 Hz (Fig. 3b). However, the sound-absorption coefficient of the 10-mm-thick natural wood starting material was ~0.02 at a frequency range of 250–2,000 Hz, which increased to 0.07 as the frequency increased to 3,000 Hz. Our results show that the delignification process greatly improves the sound-absorption coefficient of natural wood. For example, at frequencies of 500 and 2,500 Hz, the sound-absorption coefficient of insulwood is approximately ten times larger than that of natural wood (Fig. 3c).

To reveal the fundamental physics, we investigated sound propagation inside both the natural wood starting material and insulwood using finite element simulations, in which the simulated microstructures were
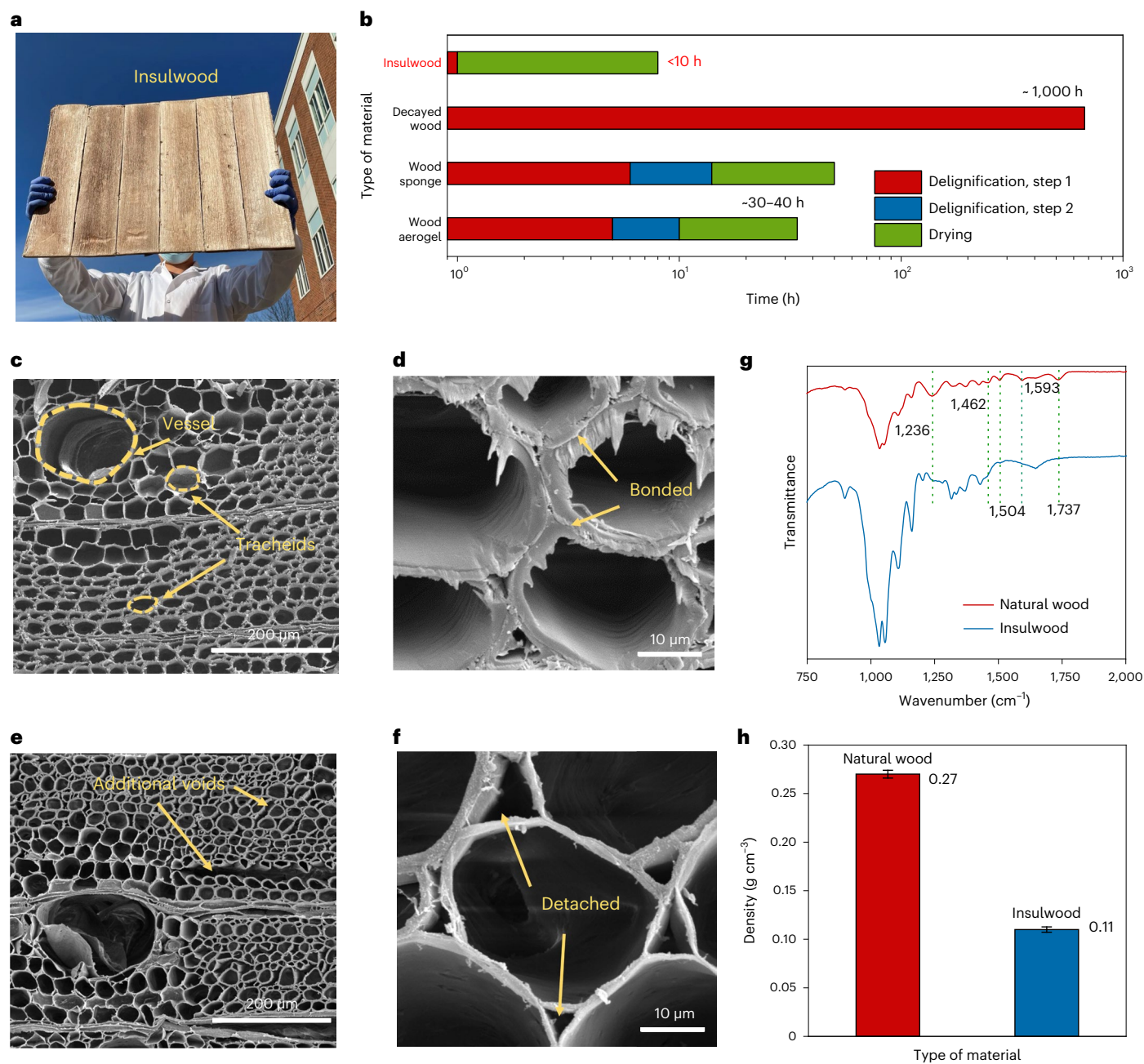
Fig. 2 | Morphology and structure of the natural wood starting material and insulwood. a, A digital image of a large-scale sheet of insulwood (60 cm × 45 cm × 1.25 cm), which is assembled from six identical smaller sheets (10.8 cm × 45 cm × 1.25 cm). **b**, Comparison of the manufacturing rates of porous wood-based structures fabricated by various top-down processes[24,25,29]. **c**, Cross-sectional SEM image of the natural wood starting material. **d**, Enlargement of **c**, demonstrating the adjacent, bonded cells in the natural wood. **e**, Cross-sectional SEM image of the insulwood. **f**, Enlargement of **e**, demonstrating the separation of the adjacent cells in the porous insulwood. **g**, FTIR spectra of the natural wood and insulwood. **h**, Density of the natural wood (0.27 ± 0.004 g cm^{-3}) and insulwood (0.11 ± 0.0028 g cm^{-3}). All data were analyzed from three independent measurements; error bars show s.d.

obtained on the basis of the scanning electron microscope (SEM) images (Supplementary Figs. 13–17). Figure 3d–i compares the distributions of the acoustic pressure and velocity as well as total thermo-viscous power dissipation within both natural wood and insulwood at a frequency of 500 Hz. Due to the rigid surface and tightly packed wood cells, the incident sound waves are reflected (Fig. 3d) and induce only very low acoustic velocity (-10^{-11} m s^{-1}; Fig. 3e) in the air within wood cells near the surface of the incident sound waves. By contrast, due to the surface cracks and micropores generated by delignification, the incident sound wave can penetrate the insulwood (Fig. 3g), causing much higher acoustic velocity (-10^{-3} m s^{-1}; Fig. 3h) in the air within insulwood. Comparison

between Fig. 3f and Fig. 3i confirms that friction between the sound waves and the walls of the detached wood cells dissipates incidence wave energy into heat. In addition, we compared the sound-absorption coefficient of the insulwood with that of other porous materials such as mineral wools and polypropylene/polystyrene foams[41–44] at 250 Hz, 500 Hz, 1,000 Hz, 1,500 Hz and 2,500 Hz (Fig. 3k). We also calculated the noise-reduction coefficient (Supplementary Fig. 17), which was the average of the sound-absorption coefficients at 250 Hz, 500 Hz, 1,000 Hz, 1,500 Hz and 2,500 Hz. Overall, the insulwood exhibits better sound absorption than various porous structures[41–44] with similar thickness in a wide frequency range.
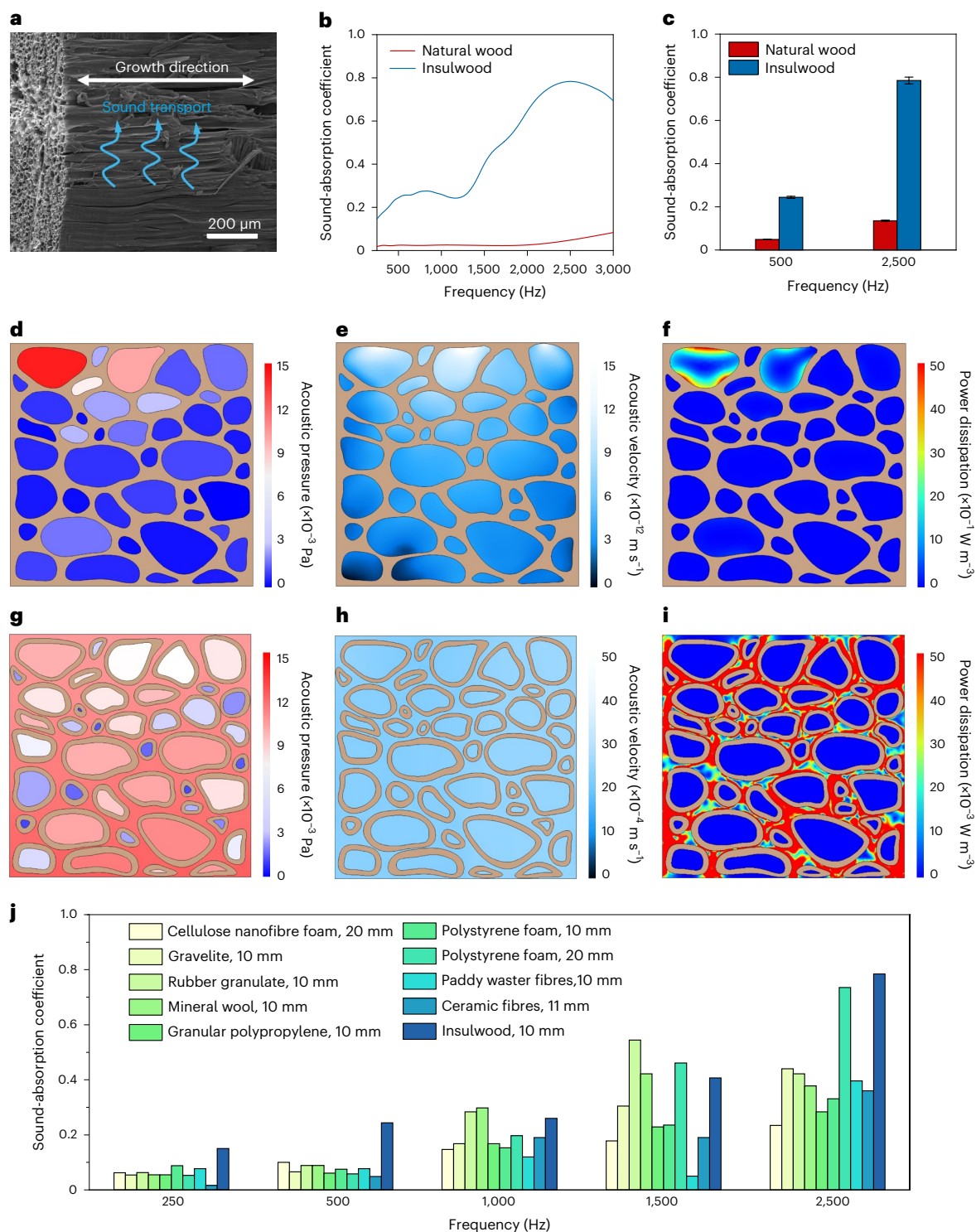
Fig. 3 | Sound absorption of the insulwood. a, SEM image of the insulwood with the pores aligned along the wood growth direction. **b**, The sound-absorption coefficient of the natural wood and insulwood as a function of frequency. **c**, The sound-absorption coefficient of the insulwood compared with that of the natural wood at frequencies of 500 Hz (natural wood: 0.05 ± 0.0001 Hz; insulwood: 0.24 ± 0.005 Hz) and 2,500 Hz (natural wood: 0.14 ± 0.003 Hz; insulwood: 0.79 ± 0.016 Hz). All data were analyzed from three independent measurements; error bars show s.d. **d–f**, Simulated distributions of the acoustic pressure (**d**), acoustic velocity (**e**) and total thermo-viscous power dissipation density (**f**)

inside the natural wood at a frequency of 500 Hz. **g–i**, Simulated distributions of the acoustic pressure (**g**), acoustic velocity (**h**) and total thermo-viscous power dissipation density (**i**) inside the insulwood at a frequency of 500 Hz. **j**, Comparison of the sound-absorption coefficients of the insulwood with various sound-absorption materials[41–44] at frequencies of 250 Hz, 500 Hz, 1,000 Hz, 1,500 Hz and 2,500 Hz. In the simulation, we assume the magnitude of the incident wave is 1 Pa, the acoustic velocity indicates particle vibration velocity in the air and the total thermo-viscous power dissipation includes the power loss through both thermal dissipation and viscous dissipation.
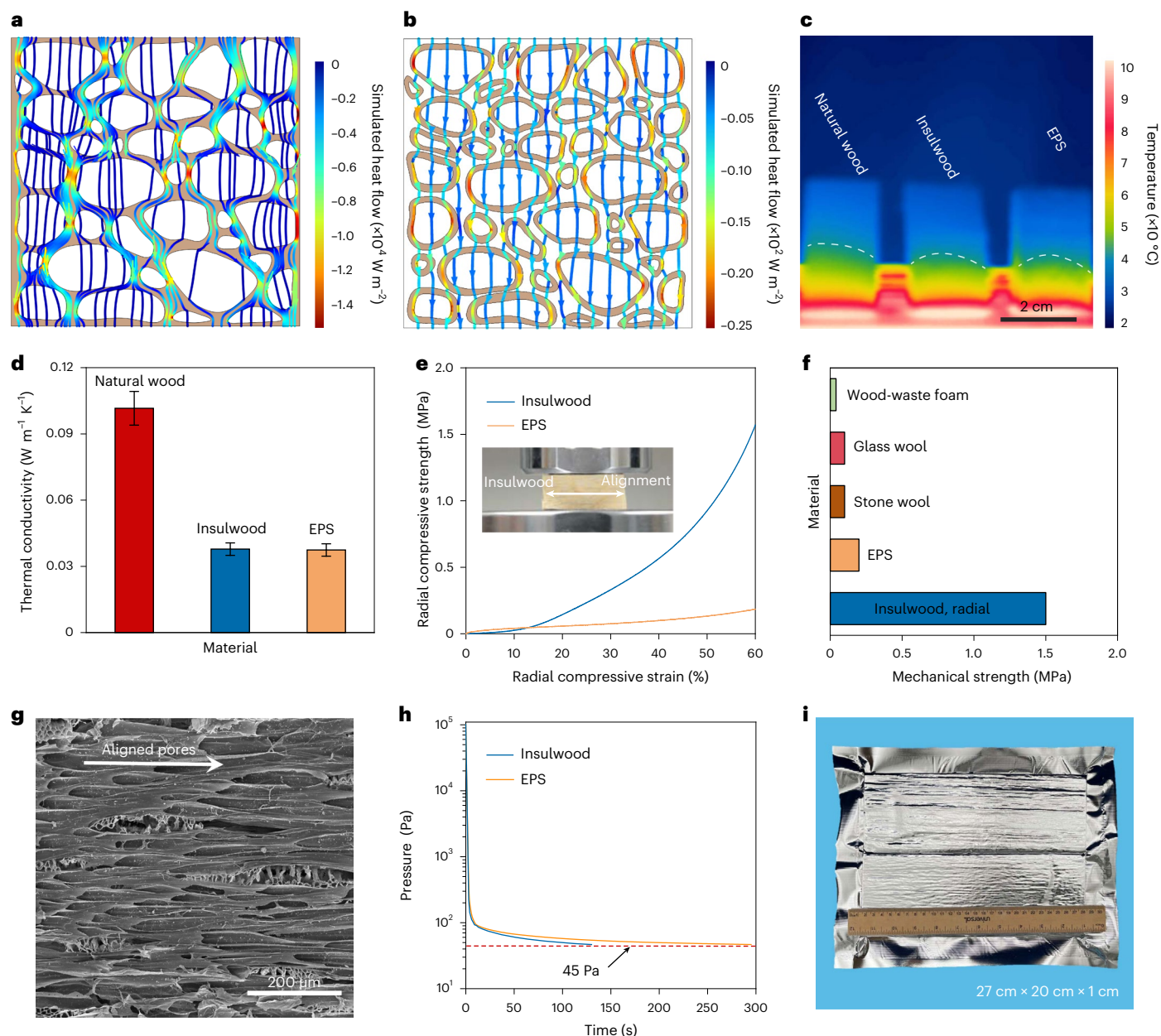
Fig. 4 | Thermal and mechanical properties of insulwood. a,b, Simulated heat flow within the natural wood (**a**) and insulwood (**b**) under a temperature difference of 2 K. **c,** Infrared image of the insulwood and EPS on a hot plate at a temperature of -100 °C. **d,** Comparison of the thermal conductivities of natural wood (0.102 ± 0.008 W m^{-1} K^{-1}), insulwood (0.0378 ± 0.003 W m^{-1} K^{-1}) and EPS (0.0374 ± 0.003 W m^{-1} K^{-1}). All data were analyzed from three independent measurements; error bars show s.d. **e,** Stress–strain curves of the insulwood under compression along the radial direction. **f,** Comparison of the mechanical strength of insulwood with conventional thermal insulation materials, including wood-waste foam[48], glass wool[49], stone wool[49] and EPS foam. **g,** SEM image of the aligned pores in the insulwood. **h,** Comparison of the outgassing rate of the insulwood with that of EPS. **i,** Image of a VIP made using insulwood as the core material.

Thermal and mechanical performance of the insulwood

Heat transfer in wood is determined mainly by heat conduction through the solid wood cell walls and the air molecules inside the pores[4]. As a result of the tightly packed wood cells and high fraction of solid content (~20%), natural wood demonstrates a relatively high thermal conductivity (0.1–0.4 W m^{-1} K^{-1} (refs. 18,20)) in the radial direction (perpendicular to the wood growth direction) compared with that of conventional porous materials (~0.035 W m^{-1} K^{-1} (ref. 45)) such as mineral wool, glass wool and expanded polystyrene (EPS) foam. Figure 4a depicts the heat flow in natural wood under a temperature difference of 2.0 K, where the thermal conductivity of the solid constructed by the wood cells and

air is assumed to be 0.34 W m^{-1} K^{-1} (ref. 46) and 0.026 W m^{-1} K^{-1} (ref. 5), respectively (Supplementary Figs. 18–20). The simulation clearly shows that heat flux through the solid (wood cell walls) is much higher than that through the air inside the pores (the interior of the wood cells), confirming that the solid conduction is responsible for the high thermal conductivity of the natural wood (Fig. 4a). Removal of the lignin and hemicelluloses in the wood cell walls lowers the solid content of the insulwood and reduces the solid thermal conductivity of the wood cell wall. As shown in Fig. 4b, heat flux through the insulwood under a temperature difference of 2.0 K is much lower than that through the natural wood due to the increased porosity. Meanwhile, the heat flux

of the insulwood is more evenly distributed than in the natural wood (Fig. 4a,b) and close to a one-dimensional heat transfer (Supplementary Fig. 19) because of the formation of pores between the wood cells after delignification.

We directly visualized the effectiveness of the insulwood as a thermal barrier by placing the material on a hot plate (~100 °C) and mapping its temperature distribution using an infrared thermal imaging camera. As shown in Fig. 4c, the temperature distribution of the insulwood (radial direction) is very similar to that of an EPS foam (~0.016 g cm^{-3}, 98.4% porosity) on the hot plate, which features a thermal conductivity of ~0.038 W m^{-1} K^{-1}. This result indicates that the thermal insulation performance of the insulwood in the radial direction is comparable to that of EPS foam. We measured the thermal conductivity of the insulwood using a reduced-scale hot-box method (Supplementary Fig. 21) developed by Zhao and co-workers[47]. As shown in Fig. 4d, the insulwood has a low thermal conductivity of ~0.038 W m^{-1} K^{-1}, which is around one-third that of the natural wood (~0.1 W m^{-1} K^{-1}). Interestingly, T the insulwood demonstrates almost the same thermal insulation performance as the EPS in terms of the temperature difference, heat flux and thermal conductivity measured by the reduced-scale hot-box method (Fig. 4d and Supplementary Figs. 21–23), which confirms that the thermal insulation performance of the insulwood in the radial direction is comparable to EPS (Fig. 4c).

While thermally insulative materials can decrease the transfer of heat, they also tend to demonstrate weak structural stability due to the high-volume fraction of pores. An important advance of our insulwood compared with conventional thermal insulators, such as EPS, mineral wool and glass wool, is its improved mechanical strength against compression. Figure 4e shows the compressive strain–stress curves of the insulwood in the radial direction. When the strain is 60% in the radial direction, the compressive strain reaches up to 1.5 MPa, which is much higher than that of conventional porous structures such as wood-waste-based foam[48], glass/stone[49] wool and EPS foam (Fig. 4e,f). In addition, due to the open pore structure of insulating materials and the chemical bonds of cellulose chains, the thermal and mechanical performance of insulwood is sensitive to moisture (Supplementary Figs. 24–26) and prone to fire. We note that these negative properties of insulwood, such as moisture resistance and fire retardancy, can be largely improved by chemical treatments such as spray coating (Supplementary Figs. 27 and 28).

As a result of the micrometre-scale pores, conventional thermal insulation materials such as EPS foams, glass wools and mineral wools and the developed insulwood exhibit a thermal conductivity higher than that of stagnant air (0.026 W m^{-1} K^{-1}, 1.0 atm, 300 K)[5,45].To achieve the required thermal insulation performance for buildings (for example, walls and roofs), conventional thermal insulation materials must have a thickness of up 50 cm (refs. 45,50), which results in reduced space and complex geometric structures. Further reduction in the thermal conductivity of porous materials can be achieved by vacuuming the porous structures to suppress gaseous thermal conduction[4,5]. VIPs are typically made of a porous core material that is evacuated then sealed by a gas-tight barrier film (for example, multilayer polymer and metal films) to achieve an ultralow thermal conductivity[50]. However, current VIPs, and particularly many of their core materials such as fumed silica nanoparticles and plastic foam cores (for example, polyurethane and EPS foams)[50], cannot meet the rising standards of sustainability and environmental safety for building applications.

As a potential substitute for conventional VIP cores, cellulose-based insulation materials have several advantages, including low cost and low environmental impact over their life cycle. In addition, the aligned channels of insulwood could enable faster evacuation during VIP manufacturing, which would dramatically reduce the gas evacuation time and energy consumption, leading to additional cost reduction (Fig. 4g and Supplementary Figs. 29 and 30). Indeed, we found that the outgassing rate of the insulwood was two times faster

than that of conventional EPS, as shown in Fig. 4h. These unique features suggest the commercial potential of insulwood-based VIPs, particularly as a more-sustainable alternative to conventional materials. As a proof of the concept, we fabricated an initial insulwood VIP design (Fig. 4i), in which the insulwood demonstrated in Fig. 2a was used as the core. The measured thermal conductivity of the fabricated VIPs at a pressure of ~50 Pa was found to be ~0.012 W m^{-1} K^{-1}, which is one-third that of the porous wood structure and half that of stagnant air (Fig. 1c). Since the gas barrier film is sound reflective and blocks the penetration of sound waves, we note that the sound-absorption coefficient of the insulwood-based VIPs is notably lower than that of insulwood.

In summary, we report a rapid, low-cost and scalable method of fabricating cellulose-based porous insulwood based on an in situ delignification, solvent exchange and ambient drying process. Lignin and hemicelluloses, which account for up to 60% of the wood mass, are removed from a natural wood via chemical treatment in just 1.0 h, which allows us to create numerous pores (voids) between the wood cell walls without destroying the hierarchically aligned cellulose fibres. As a proof of concept for large-scale production, we demonstrated the fabrication of a piece of insulwood with a size of 60 cm × 45 cm × 1.25 cm using already well-established infrastructure and equipment from the pulp and paper industry. As a result of its high porosity (~93%), the insulwood demonstrates a high noise reduction of 0.37 for frequencies at 250–3,000 Hz for a 10-mm-thick sample. The high porosity also endows the insulwood with a low thermal conductivity of 0.038 W m^{-1} K^{-1}, which is close to that of the widely used thermally insulating EPS foam. Furthermore, the porous wood structure is highly attractive for fabricating VIPs with an ultralow thermal conductivity (~0.01 W m^{-1} K^{-1}) due to the material's fast outgassing rate, sustainability and environmental safety. Compared with existing time-consuming and energy-intensive methods, our fast delignification process and ambient drying method have a higher production efficiency, lower cost and scalability. This newly developed affordable and sustainable cellulose-based insulwood with low thermal conductivity, high sound-absorption coefficient, high mechanical strength and reduced CO_2 emissions can replace conventional porous materials used in buildings, transportation and industry.

Methods
Materials and chemicals
Commercially available kiln-dried paulownia wood logs (10–15% moisture content, 10.0–12.5 mm thickness) were used for the fabrication of insulwood. Note that the moisture content of the starting wood blocks has no influence on the final properties of the insulwood. Sodium hydroxide (>97.0%, Sigma-Aldrich) and deionized water were used for processing the wood. Ethanol (>99.8%, Sigma-Aldrich) was used for solvent exchange.

Fabrication of the insulwood
A paulownia wood log was cut parallel to the growth (fibre alignment) direction to form a wood block. The wood block was then boiled in a solution of sodium hydroxide (NaOH) with a mass fraction of 5.0 wt%. The delignified wood was then washed with water to completely remove the chemical waste, bringing the pH to 7. The solvent exchange was performed by immersing the wood block in ethanol three times, each lasting for 1 h. The obtained wood blocks were then dried in an ambient environment for 7 h to achieve the final insulwood product.

Fabrication of the VIP
The insulwood blocks were first dried at 105 °C for 24 h in air to completely remove the moisture absorbed by the cellulose fibres. The dried insulwood blocks were then placed in a gas/moisture barrier envelope. After that, the VIP was obtained by pumping out the air inside the envelope with a vacuum pump (Pfeiffer HiCube 30), followed by a sealing process using an impulse heat sealer at a pressure of less than 50 Pa.

Measurements and characterizations

A SEM (Tescan XEIA) was used to characterize the morphology and structure of natural and delignified woods. A WAXS Xeuss 2.0 system with a Cu Kα (wavelength is 1.542 Å) microfocus source and Dectris Pilatus 300k detector was conducted to characterize crystal polymorphism of natural paulownia wood and insulwood. A Thermo Nicolet NEXUS 670 FTIR was used to measure the FTIR spectrum. Compression and bending tests were performed by using an Instron 3367 Universal Test System with a load capacity of 30 kN at a crosshead speed of 5 mm min^{-1}. An infrared camera FLIR E8 was used to measure the temperature distribution.

Wood composition analysis

We measured the cellulose, hemicelluloses and lignin compositions of natural woods and insulwood following the standard biomass analytical methods provided by the National Renewable Energy Laboratory[51]. To ensure that the measurements are reliable and representative of the entire wood panel, we first milled the wood panel (natural wood or insulwood) into wood powder with a diameter of <0.5 mm and mixed it evenly. Each measurement was performed three times independent of one another.

Thermal conductivity and sound-absorption measurement

We employed a reduced-scale hot box for thermal conductivity measurements[47]. Surface thermocouples (Omega, accuracy ±0.5 °C) and heat flux sensor (greenTEG gSKIN-XO, ±3%) were attached to the specimen (dimensions of 17.8 cm × 7.8 cm × 1.0 cm, ambient moisture around 50%) for surface temperature and heat-flux measurement. Steady-state conditions were ensured by controlling the power of the heat source. The thermal conductivity of the specimen can be obtained according to Fourier's law. We validated the measured thermal conductivities from the reduced-scale hot-box method by using commercial Thermtest HFM-100 and found the difference to be within 10%. The absorption test was conducted using an ACUPRO impedance tube (by TFAcoustics, LLC), which implements ISO10534-2 and ASTM E1050 for the measurement of sound-absorption coefficient as a function of frequency[40,52]. The measured samples were prepared as cylinders with a radius of 35 mm and a thickness of 10 mm. A speaker located at one end of the impedance tube broadcast a broadband white noise. The incident wave and echo reflected from the sample on the other end of the tube were measured using two microphones. On the basis of these measurements, the sound-absorption coefficient of each sample was accurately calculated in the frequency range of 250 to 3,000 Hz with steps of 6.25 Hz. The measurements were calibrated by using materials of known dissipation, and each measurement was repeated 3 times to increase the accuracy. All the measurements were performed at a similar humidity (~50%), air pressure (~1.0 atm) and temperature (~20 °C).

Reporting summary

Further information on research design is available in the Nature Research Reporting Summary linked to this article.

Data availability

The data that support the findings of this study are available within this article and its Supplementary Information. Source data are provided with this paper.

References

1. *2020 Global Status Report for Buildings and Construction: Towards a Zero-Emission, Efficient and Resilient Buildings and Construction Sector* (UNEP, 2020).
2. Cao, L., Fu, Q., Si, Y., Ding, B. & Yu, J. Porous materials for sound absorption. *Compos. Commun.* **10**, 25–35 (2018).
3. Apostolopoulou-Kalkavoura, V., Munier, P. & Bergström, L. Thermally insulating nanocellulose-based materials. *Adv. Mater.* **33**, 2001839 (2021).
4. Zhao, X., Brozena, A. H. & Hu, L. Critical roles of pores and moisture in sustainable nanocellulose-based super-thermal insulators. *Matter* **4**, 769–772 (2021).
5. Liu, H. & Zhao, X. Thermal conductivity analysis of high porosity structures with open and closed pores. *Int. J. Heat Mass Transf.* **183**, 122089 (2022).
6. Lavoine, N. & Bergström, L. Nanocellulose-based foams and aerogels: processing, properties, and applications. *J. Mater. Chem. A* **5**, 16105–16117 (2017).
7. Asdrubali, F., D'Alessandro, F. & Schiavoni, S. A review of unconventional sustainable building insulation materials. *Sustain. Mater. Technol.* **4**, 1–17 (2015).
8. Schiavoni, S., Bianchi, F. & Asdrubali, F. Insulation materials for the building sector: a review and comparative analysis. *Renew. Sustain. Energy Rev.* **62**, 988–1011 (2016).
9. Forouharmajd, F. & Mohammadi, Z. Assessment of normal incidence absorption performance of sound absorbing materials. *Int. J. Environ. Health Eng.* **5**, 10 (2016).
10. Yang, T. et al. Sound absorption properties of natural fibers: a review. *Sustainability* **12**, 8477 (2020).
11. Liu, L. et al. The development history and prospects of biomass-based insulation materials for buildings. *Renew. Sustain. Energy Rev.* **69**, 912–932 (2017).
12. Hill, C., Norton, A. & Dibdiakova, J. A comparison of the environmental impacts of different categories of insulation materials. *Energy Build.* **162**, 12–20 (2018).
13. Papadopoulos, A. M. & Giama, E. Environmental performance evaluation of thermal insulation materials and its impact on the building. *Build. Environ.* **42**, 2178–2187 (2007).
14. Xia, Q. et al. A strong, biodegradable and recyclable lignocellulosic bioplastic. *Nat. Sustain.* **4**, 627–635 (2021).
15. Esau, R., Jungclaus, M., Olgyay, V. & Rempher, A. *Reducing Embodied Carbon in Buildings* (RMI, 2021).
16. Chen, C. et al. Structure–property–function relationships of natural and engineered wood. *Nat. Rev. Mater.* **5**, 642–666 (2020).
17. Koshijima, T. & Watanabe, T. *Association Between Lignin and Carbohydrates in Wood and Other Plant Tissues* (Springer, 2013).
18. Suleiman, B., Larfeldt, J., Leckner, B. & Gustavsson, M. Thermal conductivity and diffusivity of wood. *Wood Sci. Technol.* **33**, 465–473 (1999).
19. Lin, M.-D., Tsai, K.-T. & Su, B.-S. Estimating the sound absorption coefficients of perforated wooden panels by using artificial neural networks. *Appl. Acoust.* **70**, 31–40 (2009).
20. Asdrubali, F. et al. A review of structural, thermo-physical, acoustical, and environmental properties of wooden materials for building applications. *Build. Environ.* **114**, 307–332 (2017).
21. Kang, C., Kang, W., Chung, W., Matsumura, J. & Oda, K. Changes in anatomical features, air permeability and sound absorption capability of wood induced by delignification treatment. **53**, 479–483 (Faculty of Agriculture, Kyushu University, 2008).
22. Kolya, H. & Kang, C. W. High acoustic absorption properties of hackberry compared to nine different hardwood species: a novel finding for acoustical engineers. *Appl. Acoust.* **169**, 107475 (2020).
23. Li, J., Chen, C., Zhu, J., Ragauskas, A. J. & Hu, L. In situ wood delignification toward sustainable applications. *Acc. Mater. Res.* **2**, 606–620 (2021).
24. Guan, H., Cheng, Z. & Wang, X. Highly compressible wood sponges with a spring-like lamellar structure as effective and reusable oil absorbents. *ACS Nano* **12**, 10365–10373 (2018).
25. Song, J. et al. Highly compressible, anisotropic aerogel with aligned cellulose nanofibers. *ACS Nano* **12**, 140–147 (2018).
26. Li, T. et al. Anisotropic, lightweight, strong, and super thermally insulating nanowood with naturally aligned nanocellulose. *Sci. Adv.* **4**, eaar3724 (2018).

27. Zhu, M. et al. Highly anisotropic, highly transparent wood composites. *Adv. Mater.* **28**, 5181–5187 (2016).

28. Wang, J. et al, Carbonate pre-treatment of wood for transformative structural applications through densification. *Ind Crops Prod.* **183**, 188 (2022).

29. Sun, J. et al. Enhanced mechanical energy conversion with selectively decayed wood. *Sci. Adv.* **7**, eabd9138 (2021).

30. Pour, G., Beauger, C., Rigacci, A. & Budtova, T. Xerocellulose: lightweight, porous and hydrophobic cellulose prepared via ambient drying. *J. Mater. Sci.* **50**, 4526–4535 (2015).

31. Xiao, S. et al. Lightweight, strong, moldable wood via cell wall engineering as a sustainable structural material. *Science* **374**, 465–471 (2021).

32. Ek, M., Gellerstedt, G. & Henriksson, G. *Pulping Chemistry and Technology* Vol. 2 (Walter de Gruyter, 2009).

33. Kamali, M. & Khodaparast, Z. Review on recent developments on pulp and paper mill wastewater treatment. *Ecotoxicol. Environ. Saf.* **114**, 326–342 (2015).

34. López, F., Pérez, A., Zamudio, M. A., De Alva, H. E. & García, J. C. Paulownia as raw material for solid biofuel and cellulose pulp. *Biomass Bioenergy* **45**, 77–86 (2012).

35. Yadav, N. K. et al. A review of paulownia biotechnology: a short rotation, fast growing multipurpose bioenergy tree. *Am. J. Plant Sci.* **4**, 2070 (2013).

36. Borrega, M., Tolonen, L. K., Bardot, F., Testova, L. & Sixta, H. Potential of hot water extraction of birch wood to produce high-purity dissolving pulp after alkaline pulping. *Bioresour. Technol.* **135**, 665–671 (2013).

37. Pettersen, R. C. in *The Chemistry of Solid Wood* (ed. Rowell, R.) 57–126 (ACS, 1984).

38. Kellogg, R. M. & Wangaard, F. F. Variation in the cell-wall density of wood. *Wood Fiber Sci.* **1**, 180–204 (1969).

39. Ross, R. J. *Wood Handbook: Wood as an Engineering Material* General Technical Report FPL-GTR-190 (USDA, 2010).

40. *Acoustics—Determination of Sound Absorption Coefficient and Impedance in Impedance Tubes—Part 2: Transfer-Function Method* (ISO, 1998).

41. Sikora, J. & Turkiewicz, J. Sound absorption coefficients of granular materials. *Mech. Control* **29**, 149–157 (2010).

42. Putra, A., Abdullah, Y., Efendy, H., Mohamad, W. & Salleh, N. Biomass from paddy waste fibers as sustainable acoustic material. *Adv. Acoust. Vib.* **2013**, 605932 (2013).

43. Shen, L. et al. Hierarchical pore structure based on cellulose nanofiber/melamine composite foam with enhanced sound absorption performance. *Carbohydr. Polym.* **255**, 117405 (2021).

44. Jia, C. et al. Highly compressible and anisotropic lamellar ceramic sponges with superior thermal insulation and acoustic absorption performances. *Nat. Commun.* **11**, 3732 (2020).

45. Jelle, B. P. Traditional, state-of-the-art and future thermal building insulation materials and solutions—properties, requirements and possibilities. *Energy Build.* **43**, 2549–2563 (2011).

46. Eitelberger, J. & Hofstetter, K. Prediction of transport properties of wood below the fiber saturation point—a multiscale homogenization approach and its experimental validation: part I: thermal conductivity. *Compos. Sci. Technol.* **71**, 134–144 (2011).

47. Zhao, X. et al. Reduced-scale hot box method for thermal characterization of window insulation materials. *Appl. Therm. Eng.* **160**, 114026 (2019).

48. Beluns, S. et al. From wood and hemp biomass wastes to sustainable nanocellulose foams. *Ind. Crops Prod.* **170**, 113780 (2021).

49. Chapelle, L. *Characterization and Modelling of the Mechanical Properties of Mineral Wool*. PhD thesis, Technical University of Denmark (2016).

50. Kalnæs, S. E. & Jelle, B. P. Vacuum insulation panel products: a state-of-the-art review and future research pathways. *Appl. Energy* **116**, 355–375 (2014).

51. Sluiter, A. et al. *Determination of Structural Carbohydrates and Lignin in Biomass* Technical Report NREL/TP-510-42618 (NREL, 2008).

52. *Standard Test Method for Impedance and Absorption of Acoustical Materials Using a Tube, Two Microphones and a Digital Frequency Analysis System* ASTM E1050-19 (ASTM, 2019).

Acknowledgements

Author contributions

Competing interests

The authors declare the following competing interests: Dr. Liangbing Hu co-founded a company, InventWood, to commercialize wood-based thermal/acoustic insulation materials. However, all results reported herein were performed under federal sponsorship. The remaining authors declare no competing interests.

Additional information

Supplementary information The online version contains supplementary material available at https://doi.org/10.1038/s41893-022-01035-y.

Correspondence and requests for materials should be addressed to Liangbing Hu.

Peer review information *Nature Sustainability* thanks Kai Zhang and the other, anonymous, reviewer(s) for their contribution to the peer review of this work.

Reprints and permissions information is available at www.nature.com/reprints.

Publisher's note Springer Nature remains neutral with regard to jurisdictional claims in published maps and institutional affiliations.

[1]Department of Materials Science and Engineering, University of Maryland, College Park, MD, USA. [2]Department of Mechanical Engineering, University of Maryland, College Park, MD, USA. [3]NIST Center for Neutron Research, National Institute of Standards and Technology, Gaithersburg, MD, USA. [4]InventWood LLC, College Park, MD, USA. [5]Buildings and Transportation Science Division, Oak Ridge National Laboratory, Oak Ridge, TN, USA. [6]Department of Forest Biomaterials, North Carolina State University, Raleigh, NC, USA. [7]Department of Mechanical Engineering, University of Massachusetts, Lowell, MA, USA. [8]USDA Forest Products Laboratory, Madison, WI, USA. [9]Center for Materials Innovation, University of Maryland, College Park, MD, USA. [10]These authors contributed equally: Xinpeng Zhao, Yu Liu, Liuxian Zhao. ✉e-mail: binghu@umd.edu

nature portfolio

Corresponding author(s):   Liangbing Hu

Last updated by author(s):   Nov 15, 2022

Reporting Summary

Nature Portfolio wishes to improve the reproducibility of the work that we publish. This form provides structure for consistency and transparency in reporting. For further information on Nature Portfolio policies, see our Editorial Policies and the Editorial Policy Checklist.

Statistics

For all statistical analyses, confirm that the following items are present in the figure legend, table legend, main text, or Methods section.

n/a	Confirmed	
☐	☒	The exact sample size (*n*) for each experimental group/condition, given as a discrete number and unit of measurement
☐	☒	A statement on whether measurements were taken from distinct samples or whether the same sample was measured repeatedly
☒	☐	The statistical test(s) used AND whether they are one- or two-sided *Only common tests should be described solely by name; describe more complex techniques in the Methods section.*
☐	☒	A description of all covariates tested
☐	☒	A description of any assumptions or corrections, such as tests of normality and adjustment for multiple comparisons
☐	☒	A full description of the statistical parameters including central tendency (e.g. means) or other basic estimates (e.g. regression coefficient) AND variation (e.g. standard deviation) or associated estimates of uncertainty (e.g. confidence intervals)
☒	☐	For null hypothesis testing, the test statistic (e.g. *F*, *t*, *r*) with confidence intervals, effect sizes, degrees of freedom and *P* value noted *Give P values as exact values whenever suitable.*
☒	☐	For Bayesian analysis, information on the choice of priors and Markov chain Monte Carlo settings
☐	☒	For hierarchical and complex designs, identification of the appropriate level for tests and full reporting of outcomes
☒	☐	Estimates of effect sizes (e.g. Cohen's *d*, Pearson's *r*), indicating how they were calculated

Our web collection on statistics for biologists contains articles on many of the points above.

Software and code

Policy information about availability of computer code

Data collection	COMSOL Multiphysics 5.5; No custom software was used.
Data analysis	COMSOL Multiphysics 5.5; OriginLab 8.

For manuscripts utilizing custom algorithms or software that are central to the research but not yet described in published literature, software must be made available to editors and reviewers. We strongly encourage code deposition in a community repository (e.g. GitHub). See the Nature Portfolio guidelines for submitting code & software for further information.

Data

Policy information about availability of data

All manuscripts must include a data availability statement. This statement should provide the following information, where applicable:
- Accession codes, unique identifiers, or web links for publicly available datasets
- A description of any restrictions on data availability
- For clinical datasets or third party data, please ensure that the statement adheres to our policy

The data that support the findings of this study are available within this article and its Supplementary Information. Source data are provided with this paper.

Human research participants

Policy information about studies involving human research participants and Sex and Gender in Research.

Reporting on sex and gender	*Use the terms sex (biological attribute) and gender (shaped by social and cultural circumstances) carefully in order to avoid confusing both terms. Indicate if findings apply to only one sex or gender; describe whether sex and gender were considered in study design whether sex and/or gender was determined based on self-reporting or assigned and methods used. Provide in the source data disaggregated sex and gender data where this information has been collected, and consent has been obtained for sharing of individual-level data; provide overall numbers in this Reporting Summary. Please state if this information has not been collected. Report sex- and gender-based analyses where performed, justify reasons for lack of sex- and gender-based analysis.*
Population characteristics	*Describe the covariate-relevant population characteristics of the human research participants (e.g. age, genotypic information, past and current diagnosis and treatment categories). If you filled out the behavioural & social sciences study design questions and have nothing to add here, write "See above."*
Recruitment	*Describe how participants were recruited. Outline any potential self-selection bias or other biases that may be present and how these are likely to impact results.*
Ethics oversight	*Identify the organization(s) that approved the study protocol.*

Note that full information on the approval of the study protocol must also be provided in the manuscript.

Field-specific reporting

Please select the one below that is the best fit for your research. If you are not sure, read the appropriate sections before making your selection.

☐ Life sciences   ☐ Behavioural & social sciences   ☒ Ecological, evolutionary & environmental sciences

For a reference copy of the document with all sections, see nature.com/documents/nr-reporting-summary-flat.pdf

Ecological, evolutionary & environmental sciences study design

All studies must disclose on these points even when the disclosure is negative.

Study description	Herein, we report the extraordinary noise reduction and thermal insulation capabilities of a scalable, high-porosity wood structure (called "insulwood") that is fabricated by removing lignin and hemicellulose from natural wood through a rapid high-temperature process, followed by low-cost ambient drying.
Research sample	Natural paulownia wood (density of 0.25-0.30 g/cm3) was selected as a starting material due to its fast growth rate and high biomass production (up to 50 ton/ha per year).
Sampling strategy	A paulownia wood log was cut along parallel to the growth (i.e., fiber alignment) direction to form a wood block. The wood block was then boiled in a solution of sodium hydroxide (NaOH) with a mass fraction of 5.0 wt.%, followed by solvent exchange to completely replace the water inside the wood cells with ethanol. The obtained wood blocks were then dried in an ambient environment for 7 hours to achieve the final insulwood product.
Data collection	Three samples of each material were tested to obtain the averaged values. Xinpeng Zhao carried out experiments and recorded the data. Liuxian Zhao carried out the sound absorption simulation and recorded the data. Xinpeng Zhao carried out the thermal transport simulation and recorded the data.
Timing and spatial scale	The data collection begins from April 2021 to December 2021.There is no obvious difference in the porosity, thermal and sound absorption between insulwoods made from natural paulownia wood from various locations.
Data exclusions	No data were excluded from analyses.
Reproducibility	All attempts to repeat the experiment were successful.
Randomization	All the samples were randomly tested.
Blinding	There is no blinding data collection in our work as we didn't take the ecological or medicine experiment.

Did the study involve field work?   ☐ Yes   ☒ No

Reporting for specific materials, systems and methods

We require information from authors about some types of materials, experimental systems and methods used in many studies. Here, indicate whether each material, system or method listed is relevant to your study. If you are not sure if a list item applies to your research, read the appropriate section before selecting a response.

Materials & experimental systems

n/a	Involved in the study
☒	☐ Antibodies
☒	☐ Eukaryotic cell lines
☒	☐ Palaeontology and archaeology
☒	☐ Animals and other organisms
☒	☐ Clinical data
☒	☐ Dual use research of concern

Methods

n/a	Involved in the study
☒	☐ ChIP-seq
☒	☐ Flow cytometry
☒	☐ MRI-based neuroimaging